CONTROL PROPERTIES OF NONLINEAR ACOUSTIC MATERIALS

B. D. Zaitsev, V. A. Fedorenko and I. E. Kuznetsova

**Institute of Radio Engeneering & Electronics,
Zelyonaya str.38, Saratov, Russia**

ABSTRACT

A theoretical and experimental investigation of the external electric and magnetic field influence on the bulk and surface acoustic wave characteristics in nonlinear piezoelectric, electrostrictive and piezosemiconductor materials and structures.

INTRODUCTION

Presently, acoustic devices using a controlled time delay by electric and magnetic fields are highly promising. They include acoustic phase shifters, amp- litude and phase modulators, and transversal filters with controlled amplitude – frequency characteristics. In all these units nonlinear effects are exploited which arise under propagation of acoustic waves in nonlinear materials and structures placed in external electric and magnetic fields. They are nonlinear piezoelectric, electrostrictive and piezosemiconductor materials. In this paper control acoustic properties of $LiNbO_3$, $SrTiO_3$, GaAs substrate – thin conductor layer and n Al–ZnO–n Si–Al structures are discussed.

NONLINEAR PIEZOELECTRIC AND ELECTROSTRICTIVE MATERIALS

A. NUMERICAL RESULTS FOR BAW

With a help of Green- Kristoffel equations the relative change of velocity were calculated for mechanically free and squeezed $LiNbO_3$ and $SrTiO_3$ crystals with differently oriented electric field.

For analyzes complex dependence of BAW velocity variation on the electric field intensity the control coefficients α^- and α^+ corresponding to odd and even portions were introduced. This portions were marked as follows:

$$\alpha^- = (\Delta V/V)^-/E, \qquad \alpha^+ = (\Delta V/V)^+/E^2. \quad (1)$$

Here ΔV is the velocity change due to electric field with strength E.

a. Lithium niobate

The projections of the velocity surface deformation for all wave types α^-, α^+ on the basic crystallographic planes were calculated. This projections for slow transverse waves for two planes are depicted on Fig.1 for squeezed (a) and free (b) states of crystal. It is obviously that α^-, α^+ can be either positive (solid line) or negative (dashed line).

By comparing Fig.1a and Fig.1b a certain difference in the behavior of corresponding curves is observed for the mechanically free and squeezed crystals.

The dependence of the acoustical axis Z rotation on electric field strength is shown on Fig.2.

b. Strontium titanate

In this case α^- is equal zero. The projections of the velocity surface deformation for all wave types only α^+ on the basic crystallographic planes were calculated. These projections for slow transverse waves for (001) plane and two orientations of the electric field are depicted on Fig.3 for squeezed (a) and free (b) states of the crystal. Opportunity to $LiNbO_3$ the velocity change for $SrTiO_3$ is only positive. Comparing Fig.3a and Fig.3b shows the essential difference in the behavior of corresponding curves for the mechanically free and squeezed crystals.

The dependence of the split angle of the acoustical axis [001] on electric field strength is shown on Fig.4.

B. NUMERICAL RESULTS FOR SAW

0-7803-3246-6/96/$5.00 © IEEE

The variation of Rayleigh SAW velocity was calcu-

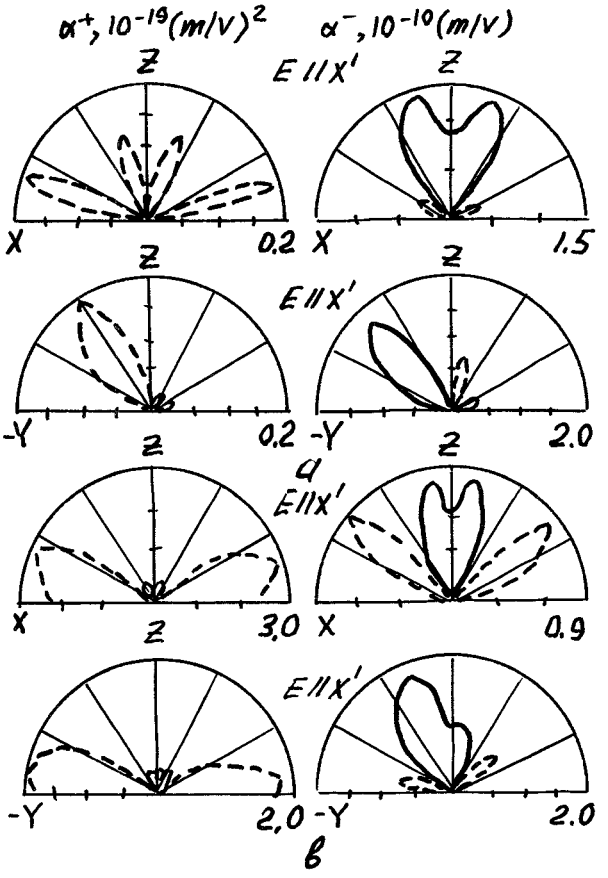

Fig. 1.

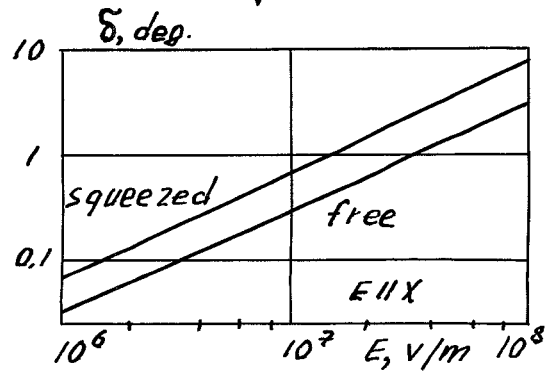

Fig. 2.

lated by the transfer matrix method for the main crystallographic axes of $LiNbO_3$ and $SrTiO_3$ under the action of differently oriented external electric fields. In this case the next situations may be considered, and namely: the crystal is mechanically squeezed or mechanically free and the surface of crystal is metallized or unmetallized.

a. Lithium niobate

Fig.5 displays the coefficients α^+ and α^- as functions of the SAW propagation direction in two crystallographic cuts for squeezed (a) and free (b) state of crystal with the unmetallized surface. The mechanical state of a crystal is seen to substantially affect electroacoustic interaction by changing its anisotropy and intensity. The control coefficient is always larger for the mechanically free crystal than for the squeezed one.

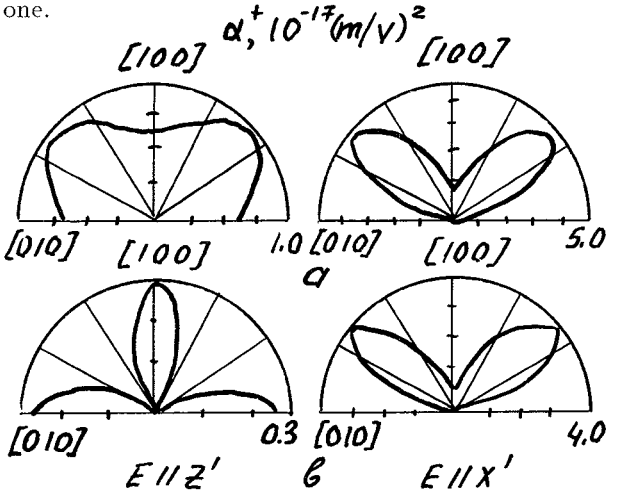

Fig. 3.

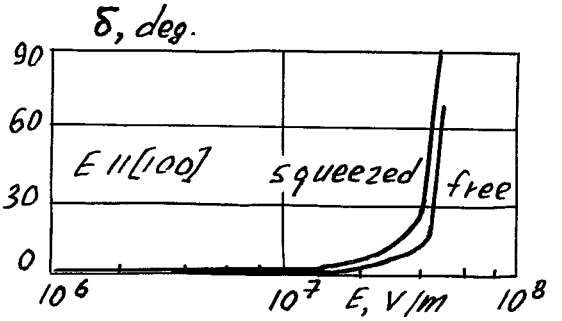

Fig. 4.

The results obtained correlate well with experimental data. This confirms by Fig.6 were our theoretical data with the experimental results of other authors [1], [2] are displayed.

b. Strontium titanate

In this case α^- is equal zero. Fig.7 displays the coefficients α^+ as functions of the SAW propagation direction in two crystallographic cuts for squeezed (a) and free (b) state of crystal with the unmetallized surface. Comparing Fig.4a and Fig.4b shows a negligible difference in the behavior of corresponding curves for the mechanically free and squeezed crystals. Theoretical conclusions are in agreement with experimentally

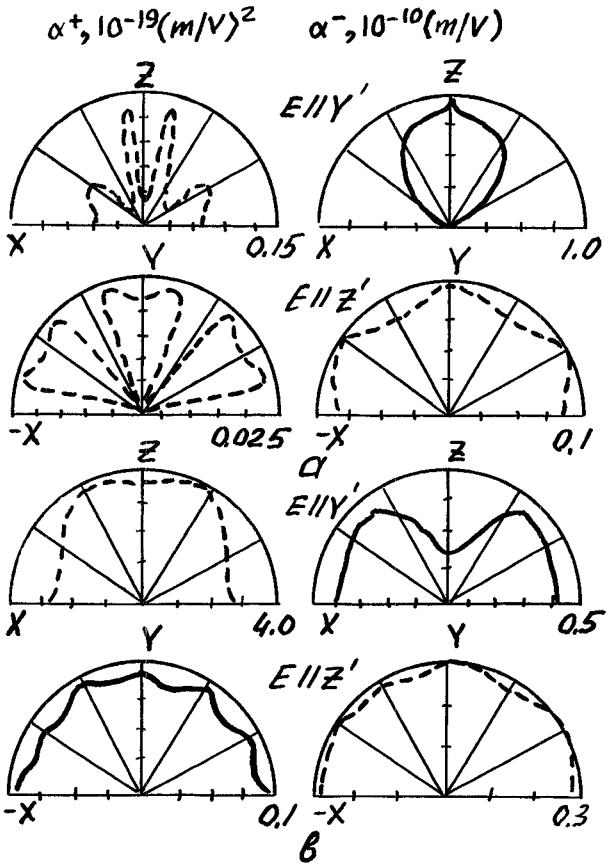

Fig. 5.

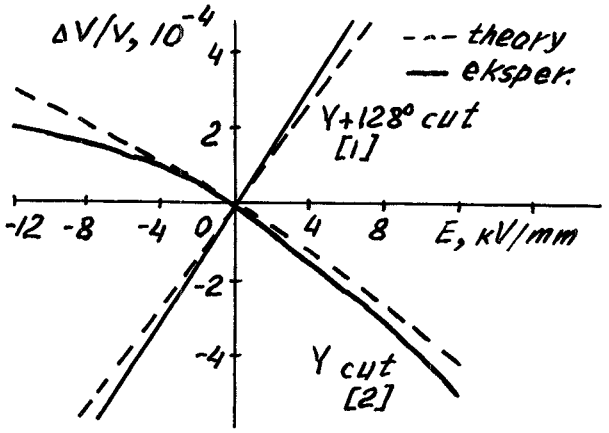

Fig. 6.

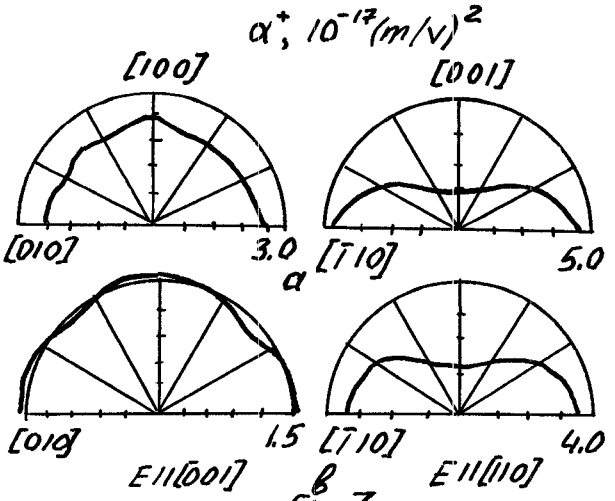

Fig. 7

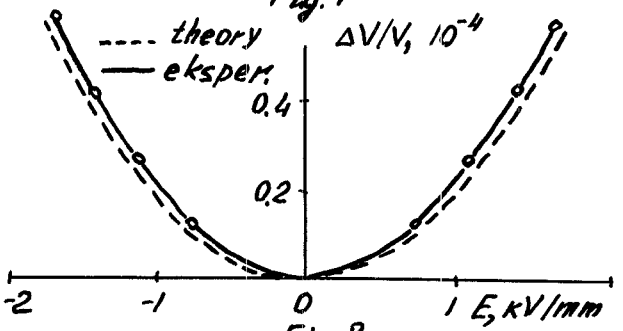

Fig. 8.

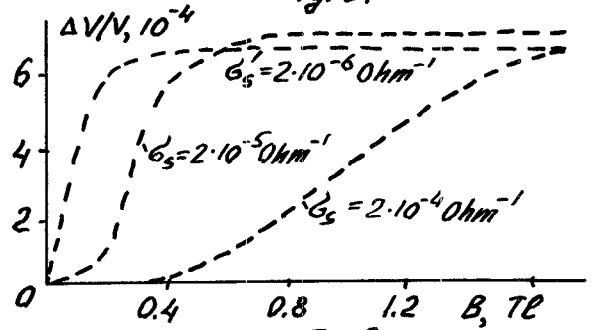

Fig. 9.

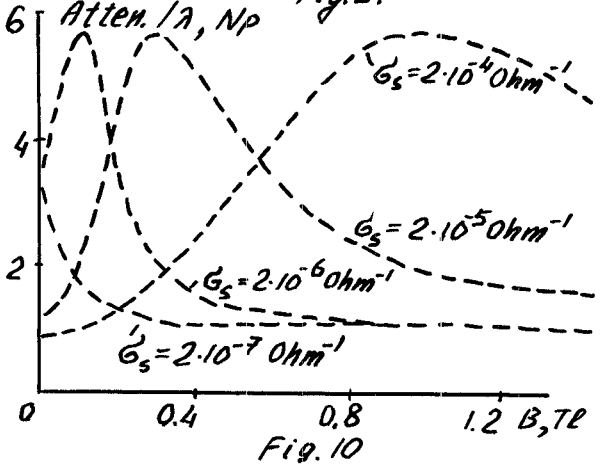

Fig. 10

found dependencies. This demonstrates by our theoretical and experimental results shown on Fig.8.

STRUCTURE OF GaAs SUBSTRATE –THIN CONDUCTIVE LAYER

Fig.9 presents the relative SAW velocity variation for structure of GaAs substrate–thin conductive layer as a function of magnetic field induction. The maximum velocity variation being equal to the electromechanical coupling coefficient insignificantly decreases with growing bulk conductivity.

The SAW attenuation and velocity for pointed structure on external magnetic field. The calculated dependencies of SAW attenuation on the magnetic field induction are indicated in Fig.10. The maximum value of attenuation may vary nearly by a factor of 5.

STRUCTURE Al–ZnO–Si–Al

In this paper we examine also the influence of constant or variable (up to the microwave band) electric voltage on the velocity of a SAW propagating in an Al–ZnO–n Si–Al structure. The SAW velocity change was measured as a function of the applied field voltage U (Fig.11, curve 1). The SAW attenuation was varied only slightly. The maximum velocity variation at $U = -10\ V$ was 0.1%. The increase of the velocity in Fig.11 (curve 1) in the region of positive fields (accumulation region) seems to be caused by the presence of trapping sites for charge carriers with a characteristic relaxation time of more than 1 s. This conclusion was bolstered by the results of an experiment with the 1 Hz sinusoidal electric voltage in the course of which the instantaneous phase variation with time was measured (curve 2 in Fig.11). This curve virtually has coincided with the appropriate dependence for the constant voltage in the depletion region (negative voltage). In the accumulation region the phase varied to only a small extent.

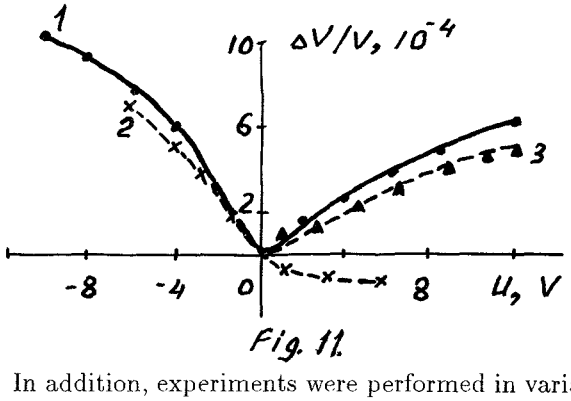

Fig. 11.

In addition, experiments were performed in variable fields at frequencies of 20 kHz and 30 GHz modulated in amplitude with a frequency of 1 Hz and the variation of the SAW average phase was recorded. The dependence $\Delta V/V(U)$ found for the frequency of 20 kHz (curve 3 in Fig.11 where the effective voltage is laid off on the U–axis) coincided with an even portion of the function $\Delta V/V(U)$ for the 1 Hz frequency. At the voltage amplitude as great as 10 V, the velocity variation made almost 0.04%. To carry out the measurements at the frequency of 30 GHz the sample was placed on the matching wedge inside a rectangular waveguide to which MW radiation was supplied. It was stated that the SAW phase was invariant with the sample heating and the dependence $\Delta V/V(U)$ (see Fig.12) practically coincided with the appropriate dependence for the frequency of 20 kHz at its initial portion.

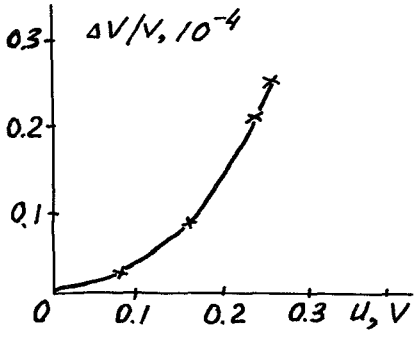

Fig. 12.

References

[1] S. G. Joshi, "Electronically variable time delay in a $LiNbO_3$ SAW delay line," *Proc.IEEE*, vol. 70, no. 1, pp. 95-96, 1982

[2] Yu. V. Gulyaev, S. S.Karinskii, V. D.Mondikov, "Investigation of external electric field influence on SAW propagation velocity in the monocrystal of $LiNbO_3$," *Pisma v ZhTPh*, vol. 1, no. 17, pp. 791-794, 1975 (in Russian)